applied sciences

MDPI

Article

Influence of Exposure to Elevated Temperatures on the Physical and Mechanical Properties of Cementitious Thermal Mortars

Manuel Cunha Pereira, António Soares, Inês Flores-Colen* and João Ramôa Correia

CERIS, Instituto Superior Técnico, Universidade de Lisboa; Av. Rovisco Pais, 1049-001, Lisbon, Portugal: mcunhapereira@gmail.com (M.C.P.); ortiz.soares@gmail.com (A.S.); joao.ramoa.correia@tecnico.ulisboa.pt (J.R.C.)

* Correspondence: ines.flores.colen@tecnico.ulisboa.pt; +351218418354

Received: 18 February 2020; Accepted: 17 March 2020; Published: 24 March 2020

Abstract: Thermal mortars incorporating insulating aggregates are a possible solution to ensure good thermal performance and thermal comfort in buildings due to their low thermal conductivity coefficient. Under some circumstances, namely for particular in-service conditions in industrial applications and/or accidental actions (such as fire), it is important to quantify the retention of their properties after exposure to elevated temperatures, however this information is not yet available in the literature. This study aims to characterize the physical and mechanical behavior of thermal mortars incorporating expanded clay, granulated expanded cork and silica aerogel as aggregates after exposure to elevated temperatures. To this end, five types of mortars were produced in laboratory conditions—three thermal mortars, one reference sand mortar and one sand mortar with admixtures—and then exposed to different elevated temperatures (from 20 °C to 250 °C) in a thermal chamber. After thermal exposure, the following properties were assessed: bulk density; ultrasonic pulse velocity; dynamic elasticity modulus; dynamic shear modulus; Poisson coefficient; compressive strength; and thermal conductivity. The results obtained show that residual properties present a very high dependence on the reactions that take place in the cement paste when the mortars are exposed to elevated temperatures. After such exposure, all mortars with thermal insulating aggregates were able to maintain their insulating characteristics, but experienced internal damage and degradation of their mechanical properties. Results obtained also showed that insulating aggregates allowed to produce mortars with higher aggregate-cement paste compatibility at elevated temperatures compared to conventional mortars, resulting in less micro-cracking of the mortar, and leading to lower reductions in thermal conductivity with increasing temperature.

Keywords: thermal mortars; insulating aggregates; elevated temperatures; mechanical behavior; thermal performance

1. Introduction

In recent years, the concern with environmental impact and thermal comfort is assuming an increasing relevance in the design and construction of buildings. The increasing demand for thermal comfort in buildings together with the energy and environmental European Directives (Directives 2002/91/EC [1] and 2010/31/EU [2]) has promoted the development of new solutions to improve the thermal performance of buildings and reduce their energy consumption. In different countries, new regulation for buildings (e.g., in Portugal, REH [3], among others) have boosted the use of new technologies for the production of innovative materials and coating systems that are able to ensure high thermal performance, without compromising their mechanical resistance. Among these solutions are thermal mortars [4], obtained through the incorporation of insulating aggregates, which

can contribute to the energy efficiency of constructions, due to their low thermal conductivity coefficient and ability to maintain coating functions [5,6].

According to European standard (EN) 998-1 [7], the maximum thermal conductivity coefficient of thermal mortars is 0.1 W/(m.K) (Class T1) and 0.2 W/(m.K) (Class T2). These mortars are also required to present minimum values of compressive strength for classes CS I (0.4 to 2.5 MPa) and CS II (1.5 to 5 MPa), capillary water absorption coefficient lower than or equal to 0.40 kg/(m^2.$min^{0.5}$) (W1 class) and water vapor permeability coefficient lower than 15.

To minimize the environmental impact and energy consumption of buildings, the performance of coating mortars can be improved by incorporating sustainable and innovative insulating [1,2,5,8] and lightweight materials [7,9–13], such as recycled aggregates and/or nanostructured materials [6,14,15]. The incorporation of insulating aggregates improves the mortars' thermal performance by significantly reducing their bulk density in the hardened state, allowing these aggregates to be classified as lightweight aggregates according to EN 206-1 and EN 13055-1, provided that their density is lower than 1200 kg/m^3 [9,10]. The present study focused on three types of thermal insulating aggregates: expanded clay, granulated expanded cork and silica aerogel.

Expanded clay combines good thermal resistance (up to 1000 °C), high porosity and low bulk density (300 to 700 kg/m^3), with high mechanical strength and low cost production, which makes it a valid solution to be used as an insulating material in construction. Expanded clay has high percentage of semi-closed pores (up to 90% of its volume), contributing to its low thermal conductivity (approximately 0.10 W/(m.K)) [16–18].

Cork is a very low density material (between 100 and 140 kg/m^3), with low thermal conductivity (0.042 to 0.070 W/(m.K)) and good mechanical properties. It is also an organic and cellular material [11,13,15]. It is used as building material because of its high physical, chemical stability and relatively low cost [12,13].

Silica aerogel is a nanostructured, extremely light and hydrophobic material characterized by an open pore structure with 95% of air content, bulk density of 3 to 500 kg/m^3, and very low thermal conductivity (0.012 to 0.021 W/(m.K)) [19–21]. The high cost and difficulty of production are presently the main obstacles to its widespread use, which is often limited to high technology applications. Silica aerogel is used not only due to its high performance as a thermal insulator, but also due to its inorganic structure; it is non-flammable and resistant up to 1400 °C [14]; according to the literature, silica aerogels slowly start to shrink from 500 °C, with the speed of the shrinking process increasing at higher temperatures. Kim et al. [22] also highlight the high stability at elevated temperatures of silica aerogels; however, in this case, for temperatures ranging from 30 °C and 1150 °C no thermal decomposition or mass changes were registered. Silica aerogel is also presented as a fire resistant material, in opposition to organic fuel foams that release toxic gases when burning [14,22].

The incorporation of silica aerogel in mortars is growing, but there are still some uncertainties concerning the mortar components (and respective content) required to obtain high thermal performance with acceptable mechanical performance [23,24]. It has been shown that the incorporation of air entrainers and rheological agents at adequate ratios allows improving the performance of thermal mortars. The air entrainers increase porosity, and the rheological agents improve the bond of the components and may also contribute to a decrease of the thermal conductivity [25,26].

It is also important that thermal mortars can maintain their properties and fulfil their initial functions during or after exposure to elevated temperatures. Several situations can cause such exposure, namely some in-service conditions in industrial applications (e.g., power stations) and/or accidental actions (e.g., fire or blast explosion) [27–29]. In those cases, it is relevant to understand the residual performance of the mortars after exposure to elevated temperatures.

Several studies addressed the effects of exposure to elevated temperatures on conventional mortars—the most relevant for the present study are highlighted next. According to Handoo [30], the exposure of cement mortars to elevated temperatures (up to 1000 °C in steps of 100 °C in a hot-air oven/muffle furnace for a soaking period of 5 h) causes material deterioration and changes in several

properties, including the loss of the cement paste binding capacity, reduction of durability, increased shrinkage on drying, structural cracking and discoloration of aggregates.

Cülfik et al. [31] studied the effects of elevated temperatures on the mechanical properties of high strength mortars. A mortar of Portland cement and sand with graphite addition (refractory material) was produced and exposed to temperatures of 300 °C, 600 °C and 900 °C without mechanical loading; the heating rate was 2 and 8 °C/min, the duration of exposure to maximum temperature was 1 and 10 h, and the cooling rate of the furnace was about 0.4 °C /min. After cooling, the mortars were subjected to compressive tests: strength reductions of about 29% and 65% were reported after exposure to temperatures of respectively 300 °C and 600 °C; for 900 °C exposure, the compressive strength was negligible. In terms of flexural strength, the mortars exhibited performance reductions of 36% and 87% after exposure to 300 °C and 600 °C, respectively. With the increase of exposure temperature, the mortars also presented increasing reductions in the static modulus of elasticity: after exposure to 300 °C the reduction was 44%. According to the authors, the main factors that influence the mechanical resistance of the mortars are (i) the thermal incompatibility between their constituents (sand has a thermal expansion coefficient of $11x10^{-6}$/°C while that of the cement paste is $16x10^{-6}$/°C), and (ii) the decomposition of the calcium hydroxide within the cement paste beyond 300°C, which causes the occurrence of internal microcracks.

Lion et al. [32] studied the effect of exposure to elevated temperatures on the properties of a conventional cement-based mortar (Portland cement CEM II B/L 32,5N) incorporating sand aggregate, namely on its porosity and gas permeability. After exposure to temperatures of 150 °C, 200 °C and 250 °C, using heating and cooling rates of 1 °C/min, and 10 h of exposure for each temperature, gas permeability and porosity tests revealed microstructural changes in the mortar, namely microcracks due to the thermal expansion of the aggregates, an increase in the number of voids due to the loss of water and increased permeability for exposure temperatures above 150 °C.

As mentioned, for some industrial applications or in the case of accidents (e.g., fire or blast explosion), mortars may be exposed to elevated temperatures. The influence of such exposure on the physical and mechanical properties of conventional cement-based mortars is reasonably well understood. Despite the actual concern about the behavior of lightweight mortars when exposed to elevated temperatures [33–35], the information about the influence of such exposure on the performance of thermal mortars is very scarce.

In order to bridge the research gap mentioned above, the present study aims at understanding the influence of exposure to elevated temperature on the residual physical and mechanical properties of cement-based thermal mortars made of expanded clay, granular expanded cork and silica aerogel lightweight insulating aggregates. In this paper different formulations of mortars were produced, then exposed to various elevated temperatures and finally subjected to a set of tests, with the following main objectives:

- To evaluate the influence of exposure to elevated temperatures on cement-based mortars with the incorporation of insulating aggregates (expanded clay, granular expanded cork, silica aerogel) and admixtures (air entrainer agent and rheological agent);
- To study the influence of exposure to elevated temperatures in the different mortars produced, namely on the following physical and mechanical properties: bulk density; ultrasonic pulse velocity; dynamic elasticity modulus; dynamic shear modulus and Poisson coefficient; compressive strength and thermal conductivity;
- To compare the behavior of the different mortars and understand the effects of exposure to elevated temperature on their performance and on the correlations between the most affected properties.

2. Materials and Methods

Five types of mortars were produced: three thermal mortars, containing 100% of expanded clay (A^{EC} mortar) with bulk density of 550 kg/m^3 and Euroclass A1 of reaction to fire; 100% of granular expanded cork (B^{GEC} mortar) with bulk density of 55 kg/m^3 and thermal conductivity of 0.039 W/(m.K); or 100% of a commercial silica aerogel (C^{AERO} mortar) with bulk density between 80 and 100

kg/m^3 and thermal conductivity between 0.01 and 0.031 W/(m.K); one reference mortar (D^{ref} mortar) based on silica sand with bulk density of 1520 kg/m^3; and one silica sand mortar (E^{AD} mortar) with admixtures (anionic surfactant (Hostapur OSB) as air entrainer agent, and methyl-hydroxyethyl-cellulose as rheological agent). The aggregate properties mentioned above are the ones provided by the manufacturers datasheets (expanded clay 0-2 from Argex; expanded cork from Amorim; Lumira aerogel PS100 particles from Cabot; and APAS 60 sand from Areipor).

The composition of each mortar is shown in Table 1. The water/cement ratios were based on EN 1015-2 [36] flow value parameters for bulk density of fresh mortar on mortars without admixtures. Since the standard EN 1015-3 [37] does not include the use of admixtures in its scope of use, for mortars with admixtures the water/cement ratios were the ones that allowed a good workability for each mortar. The water/cement ratios for mortars without admixtures were defined according to flow value parameters for bulk density of fresh mortar in line with EN 1015-2 [36]. Since the standard EN 1015-3 [37] does not include the use of admixtures in its scope of use, the water/cement ratios for mortars with admixtures were the defined in order to ensure a good workability for each mortar, namely providing a flow value similar to that required by standard EN 1015-2.

Table 1. Composition of the mortars produced.

Mortar	Aggregate	Cement binder	Water/cement ratio	Aggregate size [mm]	Admixtures [%]	
					Air entrainer agent	Rheological agent
A^{EC}	Expanded clay	CEM II 32.5N	0.90	0.5 to 2.0	-	-
B^{GEC}	Granular expanded cork		1.00		-	-
C^{AERO}	Silica aerogel		0.90		0.5	0.075
D^{REF}	Sand		0.65		-	-
E^{AD}			0.55		0.5	0.075

An aggregate to water volumetric ratio of 1:4 was used for the production of all mortars, a very common ratio for conventional cement-based mortars [38]. In addition, the same binder was used in all mortars—Portland cement type CEM II B/L 32.5 N.

In total, five batches were produced for each mortar, each one for a given target exposure temperature. The particle grading sizes used for the studied mortars were selected with fraction sizes from 0.5 to 1 mm and from 1 to 2 mm, in agreement with the grain sizes of the thermal insulating aggregates. For each mortar, five prismatic samples measuring 160×40×40 mm^3 were produced for mechanical strength tests (except for mortar C^{AERO}, for which 3 prismatic samples were produced) and two cylindrical samples with 60 mm of diameter and 20 mm of thickness were produced for thermal conductivity measurements.

All the samples were stored and cured according to the EN 1015-11 standard [39]: they were first cured in polyethylene bags (7 days) and then subjected to dry curing (21 days) in a climatic chamber under controlled conditions of 20 °C ± 2°C and relative humidity of 65% ± 5%.

After removal from the molds and completion of the curing process, the samples were exposed to the following elevated temperatures inside a Tinius Olsen ventilated thermal chamber: 100 °C, 150 °C, 200 °C and 250 °C. Each batch of mortar specimens was heated at a rate of 2.5 °C/min (air temperature inside the thermal chamber) up to the target temperature, which was kept constant during a soaking period of 1 hour (to ensure thermal equilibrium in the specimens), and then cooled to ambient temperature at a rate of −1.5 °C/min; these relatively low heating/cooling rates aimed at minimizing the internal stresses due to temperature gradients (Figure 1). Before being subjected to the different characterization tests (described below), the specimens were placed back in the climatic chamber for 24 hours.

Figure 1. Thermal chamber before the tests.

The following physical and mechanical properties of the mortars at room temperature (reference condition) and after exposure to elevated temperatures were assessed: bulk density, ultrasonic pulse velocity, Young's modulus, dynamic shear modulus, Poisson ratio, compressive strength, and thermal conductivity. The compressive strength was indirectly estimated based on the values of the Young's modulus [40]. In particular, the relationship between those two properties obtained by Silva et al. [41,42] was considered. The main procedures of these tests, performed according to European and American standards [40,43–45], are described next.

The bulk density of the mortars in the hardened state was determined by the geometrical principle established in EN 1015-10 [43], based on the measurement of the actual dimensions of each specimen (considering the average of three measurements) and of its weight using a scale with an accuracy of ± 0.1 g. The bulk density can be readily calculated based on the volume and mass values of the test specimens.

The ultrasonic pulse velocity test was performed on prismatic specimens according to EN 12504-4 [44]. Although this standard was developed for concrete, it is also applicable to mortars. A Proceq Pundit Lab + equipment was used, connected to two 54 kHz frequency transducers; vaseline (a blend of mineral oils and waxes) was applied as contact material at the interfaces between the test specimens and the two transducers.

The Young's modulus was determined in prismatic specimens as specified in American Society for Testing and Materials (ASTM) standard E1876-01 [40] (non-destructive test), using a GrindoSonic MK5 "Industrial" equipment. This equipment consists of a sensor and an electronic system that captures the resonant frequency of the test specimen, placed on supports located at the fundamental nodal points, that vibrates due to the strike of a drumstick (Figure 2).

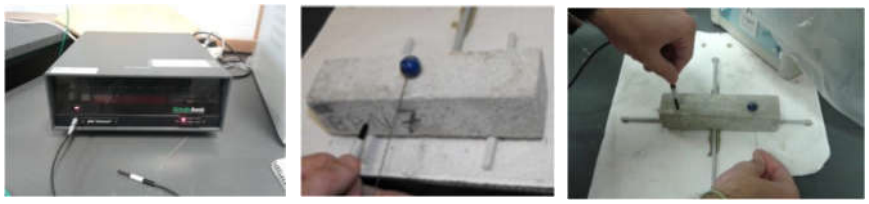

Figure 2. GrindoSonic MK5 equipment (left); test to obtain flexural vibration frequency (center); test to obtain torsional vibration frequency (right).

An Isomet 2114 equipment [45,46] was used to determine the thermal conductivity of the specimens, following the ASTM standard D5930-09 standard. The test was performed using a surface probe placed on the surface of the specimen, which analyses the thermal response to thermal impulses transmitted by the probe. The tests were performed on the cylindrical specimens (diameter of 60 mm and thickness of 20 mm). In these tests, the surface of the test specimens should be as flat as possible in order to maximize the contact surface with the probe. In order to minimize the effect of abrupt temperature and ambient humidity variation, the test specimens were wrapped in adherent

film and placed on an EPS plate 12 h prior to the test, for a dry state test at ≈ 20 °C. Due to limitations of the available materials, this test was only performed for the control temperature, 150 °C and 250 °C.

3. Results and Discussion

This section presents and discusses the results obtained from the experimental tests, namely the bulk density at hardened state (ρ); the ultrasound pulse velocity (UPV); the dynamic elasticity modulus (E_d); the dynamic shear modulus (G_d); the Poisson coefficient (ν); the compressive strength (f_c, estimated from E_d); and the thermal conductivity (λ).

It is worth mentioning that during the heating of the mortars exposed to higher temperatures (150°C, 200°C and 250°C), the occurrence of condensation inside the thermal chamber was observed. This condensation occurred due to the evaporation of water from the specimens [32].

3.1. Bulk Density

Prior to heat exposure, the bulk density in hardened state (ρ) of the various mortars ranged between 432 and 737 kg/m³ for mortars incorporating insulating aggregates and between 1590 and 1730 kg/m³ for sand mortars; these significant differences highlight one of the main features of the former mortars—lightweight.

For the temperature range studied, exposure to elevated temperatures influenced the bulk density of the mortars in the hardened state (Figure 3 and Table 2), with variations around 10%, except for the silica aerogel mortar (C^{AERO}), whose bulk density presented a reduction of about 25% for the temperature of 250 °C. According to EN 998-1 [7], these thermal mortars can be classified as lightweight mortars (before and after heat exposure), since their bulk density is (considerably) lower than 1300 kg/m³.

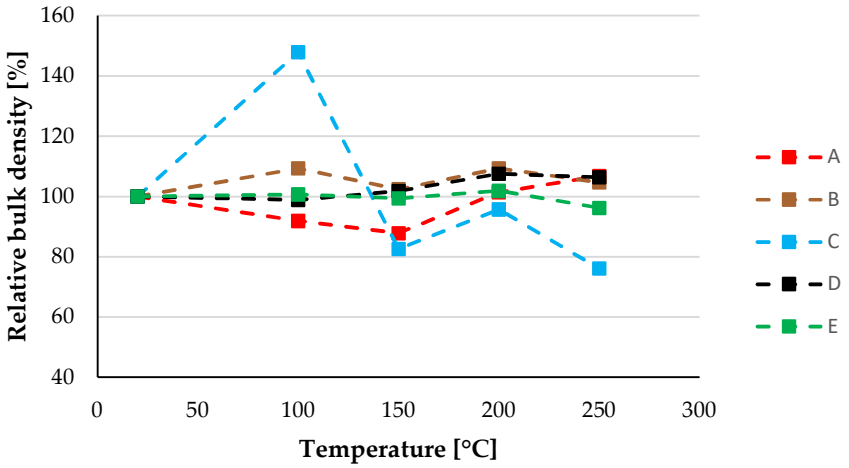

Figure 3. Bulk density (%) vs. exposure temperature.

Table 2. Bulk density average vs. exposure temperature.

Bulk density [kg/m³] (standard deviation)						
Mortar		**A**	**B**	**C**	**D**	**E**
Temperature [°C]	20	740 (22)	430 (13)	460 (7)	1730 (31)	1590 (25)
	100	680 (12)	470 (20)	680 (13)	1710 (29)	1600 (23)
	150	650 (24)	440 (16)	380 (8)	1760 (23)	1580 (42)
	200	750 (7)	470 (7)	440 (5)	1860 (25)	1620 (15)
	250	790 (21)	450 (24)	350 (8)	1840 (11)	1530 (30)

In sand mortars (D^{ref} and E^{AD}) no significant variations in density were observed up to 100 °C. Between 100 °C and 150 °C there was a reduction in density that can be explained by the evaporation of water from the cement paste [47], chemically combined (starting from 105 °C) and in small pores (starting from 120 °C) [48,49], and by a probable internal expansion of cement paste [50,51]. Around 150 °C, the cement paste undergoes a strong shrinkage due to dewatering, which may justify the increase of the density of these mortars beyond 150 °C [50,52,53]. In addition, rising temperatures above 100 °C may lead to the production of various forms of calcium silicates, which although generally porous and weak, may also justify increased density [48]. Mortars D^{ref} and E^{AD} present similar variation in density with temperature change (especially after 100 °C), indicating that the used admixtures do not affect the influence of temperature on mortar bulk density.

Despite the increase in density of aerogel mortar (C^{AERO}) at 100 °C, probably related to the initial hydration products formed at elevated temperatures [54], after 150 °C this mortar showed the same pattern of variation as the other ones. The mortar with cork (B^{GEC}) also followed the trend of C^{AERO} mortar. However, this mortar showed a better density stability with the temperature increase, with a maximum variation of 40 kg/m^3 (≈9% of the initial mass).

For the expanded clay mortar (A^{EC}) the density also increased for exposure temperatures higher than 150 °C. However, up to 150 °C, compared to other mortars, there was a more constant decrease in the density of expanded clay mortar, which may be related to the higher porosity of expanded clay—this allows greater water movement than in more compact materials [48], possibly leading to an earlier water evaporation than in the other mortars.

3.2. Ultrasonic Pulse Velocity

The strength of a mortar can be estimated based on the principle that more compact materials present higher wave propagation speeds and resistance values. Therefore, with the ultrasonic pulse velocity (UPV) test, it is possible to assess the compactness of mortars and consequently its state of internal degradation (discontinuities, voids). As expected, prior to heat exposure the values of the UPV of thermal mortars were lower than those of sand mortars. As depicted in Figure 4 and Table 3, exposure to elevated temperatures had a reduced influence in the UPV of the expanded clay (A^{EC}) and granular expanded cork (B^{GEC}) mortars.

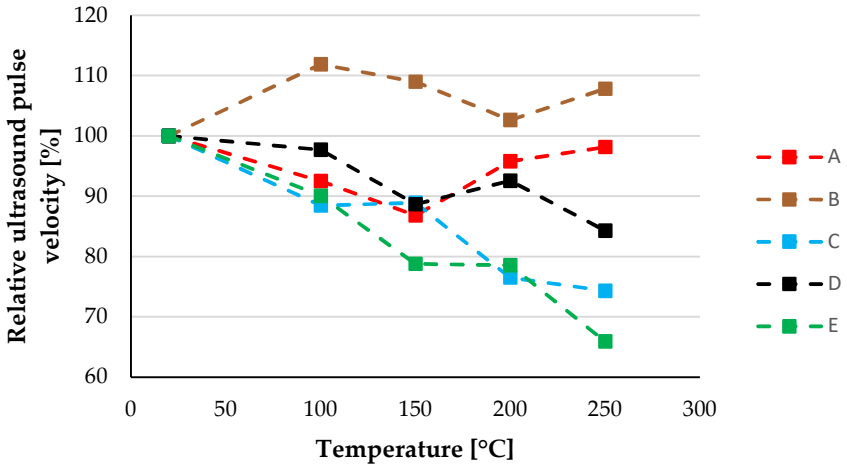

Figure 4. Ultrasound pulse velocity (%) vs. exposure temperature.

Table 3. Ultrasound pulse velocity average vs. exposure temperature.

Ultrasound pulse velocity [m/s] (standard deviation)						
Mortar		**A**	**B**	**C**	**D**	**E**
Temperature [°C]	20	2379 (64)	994 (48)	1094 (7)	3081 (39)	2551 (38)
	100	2201 (28)	1112 (41)	968 (30)	3010 (155)	2298 (77)
	150	2065 (26)	1083 (27)	973 (1)	2732 (34)	2010 (57)
	200	2279 (58)	1020 (48)	837 (38)	2852 (68)	2003 (33)
	250	2335 (71)	1072 (42)	813 (26)	2597 (115)	1681 (130)

The silica aerogel mortar (C^{AERO}) was sensitive to high temperatures, with a reduction of UPV of 25% after exposure to 250 °C. After exposure to elevated temperature, sand mortars also experienced UPV reductions, mainly for the mortar with admixtures (above 100 °C), with a maximum reduction of 34% (E^{AD}) after exposure to 250 °C. The reduction of UPV after heat exposure in both insulating and conventional mortars may reflect the development of mortar discontinuities, namely increasing porosity and micro-cracking [33].

3.3. Young's Modulus, Dynamic Shear Modulus, Poisson Ratio and Compressive Strength

Regarding the influence of elevated temperature on the Young's modulus (Figure 5 and Table 4), for the silica aerogel mortar (C^{AERO}), it started to decrease for temperatures above 200°C, with a reduction of 37% for 250 °C. With the increase of the exposure temperature, the Young's modulus of the expanded clay (A^{EC}) and reference (D^{ref}) mortars showed reductions between 17% and 29%, and between 5% and 20%, for 200 °C and 250 °C, respectively. The Young's modulus of granular expanded cork mortar (B^{GEC}) increased, possibly due to the effect of the straightening of the cork cells' walls, influenced by high temperatures [55]. As for the mortar with admixtures (E^{AD}), it showed reduced susceptibility up to 100 °C, but for higher temperatures, the Young's modulus reduced between 29% and 55%. In general, the dynamic shear modulus and Poisson ratio (summarized in Table 5) presented similar behavior to the Young's modulus, generally decreasing with the increase of the exposure temperature. The decrease of Young's modulus between 200 °C and 250 °C, in almost all mortars (only exception to $A^{EC)}$ is in line with the results of Phan [56] who obtained more brittle ruptures at 200 °C than at higher temperatures. This behavior can be associated to increased thermal stresses and physical and chemical changes in mortar microstructure [57].

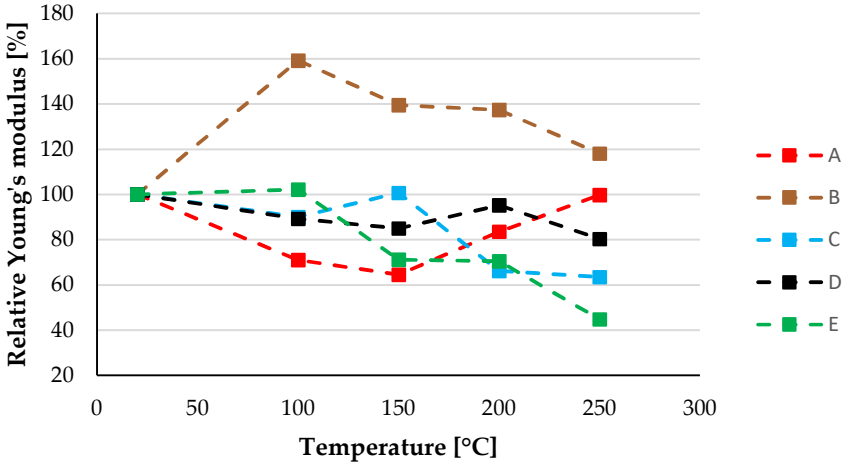

Figure 5. Young's modulus (%) vs. exposure temperature.

Table 4. Young's modulus average vs. exposure temperature.

Young's modulus [MPa] (standard deviation)						
Mortar		**A**	**B**	**C**	**D**	**E**
Temperature [°C]	20	3152 (285)	238 (30)	290 (17)	12310 (815)	6944 (495)
	100	2239 (122)	379 (61)	261 (3)	10984 (908)	7095 (1053)
	150	2033 (176)	332 (52)	292 (5)	10454 (643)	4939 (481)
	200	2631 (65)	327 (21)	192 (8)	11718 (564)	4890 (243)
	250	3144 (279)	281 (31)	184 (10)	9891 (133)	3111 (465)

Table 5. Summary of dynamic shear modulus and Poisson ratio: average and standard deviation (in parentheses).

Properties	**Temperature [°C]**	**Mortar**				
		A	**B**	**C**	**D**	**E**
Dynamic shear modulus [MPa]	20	1349 (71)	98 (14)	66 (4)	2826 (139)	3230 (97)
	100	955 (82)	124 (45)	122 (2)	3369 (1091)	3000 (317)
	150	888 (68)	128 (46)	64 (2)	2606 (411)	2223 (179)
	200	1177 (35)	140 (10)	99 (4)	5213 (180)	2178 (57)
	250	1379 (137)	99 (29)	86 (1)	4455 (110)	1387 (324)
Poisson ratio [–]	20	0.17 (0.05)	0.23 (0.16)	0.30 (0.00)	0.30 (0.00)	0.13 (0.11)
	100	0.18 (0.08)	0.29 (0.02)	0.08 (0.01)	0.24 (0.09)	0.18 (0.06)
	150	0.15 (0.06)	0.20 (0.12)	0.30 (0.00)	0.30 (0.00)	0.11 (0.03)
	200	0.12 (0.02)	0.17 (0.07)	0.30 (0.00)	0.12 (0.04)	0.12 (0.05)
	250	0.14 (0.04)	0.31 (0.10)	0.16 (0.12)	0.11 (0.04)	0.05 (0.02)

Analyzing the compressive strength (indirectly obtained from a non-destructive method and the correlation with the Young's modulus [41], through the equation $f_c = 0.0364 \times E_d 0.5832$, a $R^2 = 0.9992$), the reduction in compressive strength between 100 °C and 150 °C for almost all mortars (Figure 6 and Table 6) can be explained by the partial damage of cement paste due to water release at 105 °C and also to ettringite and C-S-H gel dehydration. When water evaporates, the build-up of internal pore pressure may induce significant internal stresses on the solid skeleton of the mortar [48].

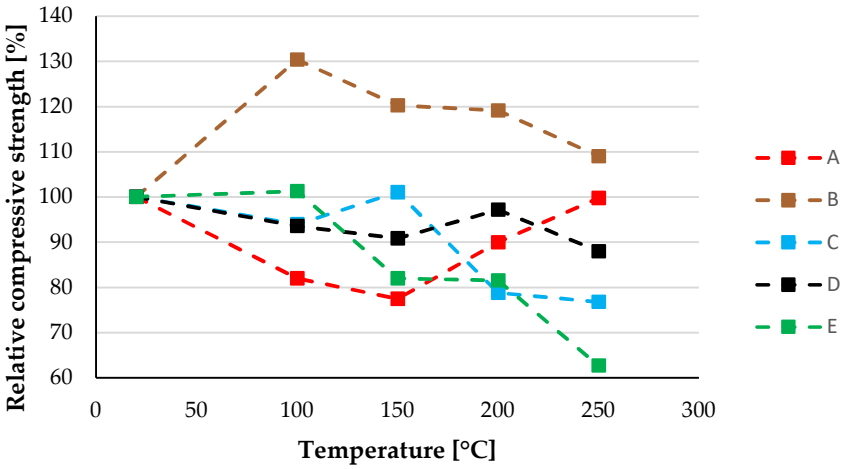

Figure 6. Compressive strength (%) vs. exposure temperature.

Table 6. Compressive strength average vs. exposure temperature.

Compressive strength [MPa] (standard deviation)						
Mortar		**A**	**B**	**C**	**D**	**E**
Temperature [°C]	20	3.99 (0.19)	0.89 (0.06)	0.99 (0.03)	8.83 (0.31)	6.32 (0.24)
	100	3.27 (0.09)	1.16 (0.10)	0.93 (0.01)	8.26 (0.36)	6.40 (0.49)
	150	3.09 (0.14)	1.07 (0.09)	1.00 (0.02)	8.02 (0.26)	5.18 (0.27)
	200	3.59 (0.05)	1.06 (0.04)	0.78 (0.03)	8.58 (0.22)	5.15 (0.14)
	250	3.98 (0.18)	0.97 (0.06)	0.76 (0.02)	7.77 (0.06)	3.96 (0.31)

Between 150 °C and 200 °C there was an increase in compressive strength in mortars A^{EC} and D^{ref} and stabilization in mortars B^{GEC} and E^{AD}. This behavior is due to the competing effects of acceleration of hydration of the non-hydrated cement and degradation due to microcracking [49]. This hydration results from the passage of water vapor released by the pores originating steam condition under the effect of the so-called internal autoclaving that occurs from 160 °C to 220 °C in cement-based materials [58,59]. After 200 °C, decomposition of C-S-H gel and the sulfoaluminate phase cause cracks with significant effect on the compressive strength [60].

Despite de the considerable relative variation, the smaller variation of the compressive strength (in absolute value) of expanded clay mortar compared to sand mortars may be justified by a greater compatibility of the coefficient of thermal expansion (CET) of cement paste with that of expanded clay when compared to sand [50]. The different magnitudes of the compressive strength changes point out the importance of considering the CET of the aggregates in mortars exposed to elevated temperatures.

Thus, when analyzing the variation in compressive strength with increasing temperature, the largest variations (1.06 MPa in mortar D^{ref} and 2.44 MPa in mortar E^{AD}) occurred in mortars with sand (with CET between 10 and 13 × 10-6 $°C^{-1}$ [61]), followed (0.9 MPa) by the AEC mortar with expanded clay (with CET between 6 and 10 × 10-6 $°C^{-1}$ [61]).

The mortar with the lowest variation in compressive strength (0.24 MPa) was the C^{AERO} mortar with silica aerogel, which has the lowest CET (between 2 and 4 × 10-6 $°C^{-1}$ [62]) among all aggregates under study. Although granulated expanded cork has a high CET (between 25 and 50 × 10-6 $°C^{-1}$ [63]), it also has a high compressibility [64], which may explain the small variation in compressive strength (0.27 MPa) of mortar B^{GEC}.

Thus, the major effects (reduction and increase in density and mechanical resistance) caused by increasing temperature are essentially due to the temperature influence on the cement paste. This study shows that the magnitude of those effects depends significantly on the types of aggregates, namely their thermal expansion coefficient and compressibility.

After exposure to high temperatures, and despite the change of some mechanical characteristics, the thermal mortars studied showed compressive strength values between 0.76 MPa and 3.98 MPa, being classified as CS I and CS II mortars, thus still complying with the EN 998-1 standard applied for thermal mortars [7].

3.4. Thermal Conductivity

In terms of thermal performance, after exposure to 250 °C, all mortars suffered a thermal conductivity reduction (Figure 7 and Table 7). This variation should be associated with possible changes in the internal structure of the mortars, namely the increasing porosity and micro-cracking. This reduction was more pronounced in sand mortars (mainly in mortar D^{ref}), indicating a greater micro-cracking of these mortars. These results are in line with those previously discussed, where the properties of these mortars were reported to present a greater variation due to a higher aggregate / paste incompatibility under thermal expansion caused by temperature increase.

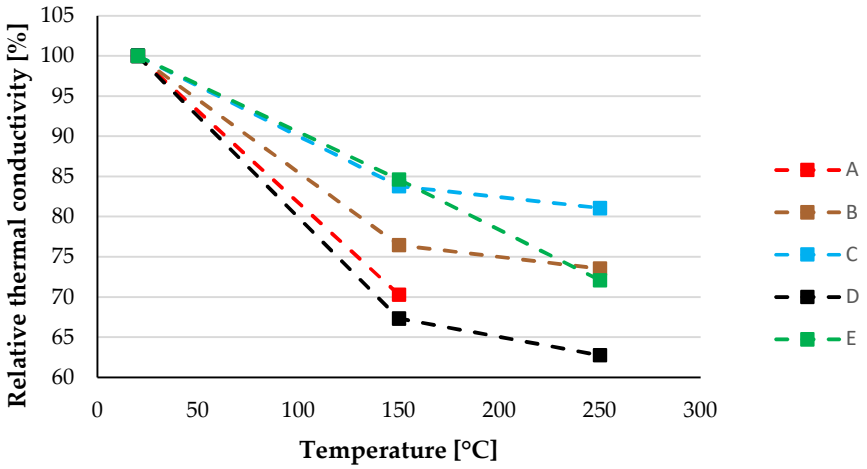

Figure 7. Thermal conductivity coefficient (%) vs. exposure temperature.

Table 7. Thermal conductivity coefficient (average) vs. exposure temperature.

Thermal conductivity [W/(m.K)] (standard deviation)						
Mortar		**A**	**B**	**C**	**D**	**E**
Temperature [°C]	**20**	0.202 (0.002)	0.102 (0.005)	0.074 (0.000)	1.987 (0.009)	1.326 (0.010)
	150	0.142 (0.001)	0.078 (0.007)	0.062 (0.001)	1.338 (0.051)	1.122
	250	0.040*	0.075	0.060	1.247	0.956 (0.359)

* This is a very low value for this mortar since the aggregate expanded clay exhibits a thermal conductivity around 0.1 W/(m.K) [16]. For this reason, this value was excluded from the remaining analysis.

The lightweight aggregates, with better compatibility with the cement paste under expansion phenomena, enable the mortar to maintain thermal insulation properties with acceptable thermal conductivity values. This is quite clear in mortars B^{GEC} and C^{AERO}, for which the thermal conductivity variation is 0.027 and 0.014 W/(m.K), respectively.

After exposure to 250 °C, the mortars with thermal insulating aggregates (silica aerogel and granular expanded cork (GEC)) presented a thermal conductivity coefficient between 0.06 W/(m.K) and 0.075 W/(m.K); therefore, since their thermal conductivity coefficient is below 0.1 W/(m.K), they comply with thermal class "T1" for thermal mortars according to standard EN998-1 [7], even after being exposed to high temperatures.

3.5. Correlations between Physical and Mechanical Properties

To provide a better understanding of the influence of high temperatures in the different properties of the mortars, correlations between physical and mechanical properties were established. For that purpose, individual values obtained from each sample were used in order to directly compare two properties (for example: the correlation between UPV and bulk density values for the same specimen, at a specific temperature, corresponds to a scatter point in Figure 8).

It is possible to relate the values of UPV and bulk density in the hardened state, because both properties depend on the characteristics of the material, i.e., a material with weaker cohesion will also have lower UPV and vice versa [65,66]. In Figure 8 it is possible to observe the relation between the UPV and bulk density of the various mortars for the different exposure temperatures.

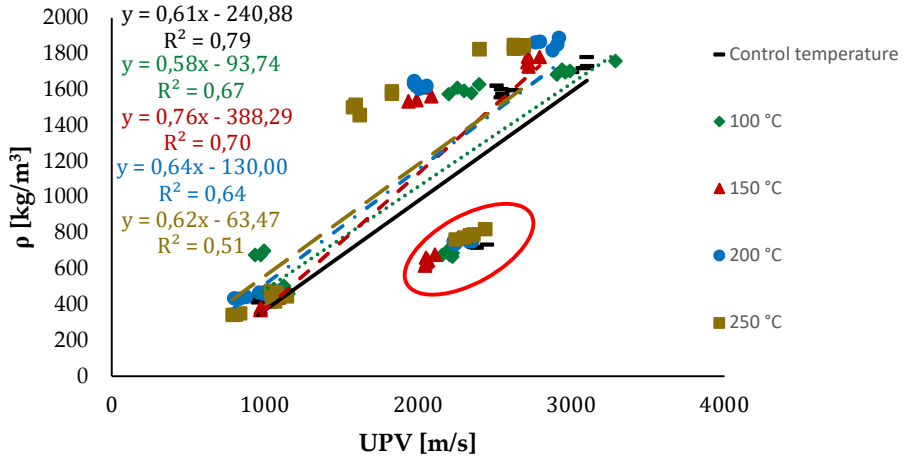

Figure 8. Relationship between ultrasound pulse velocity and bulk density.

Acceptable linear tendencies were obtained, with correlation coefficients of Pearson ranging between 0.64 and 0.79 for mortars exposed to temperatures up to 200 °C, which decreased with the temperature increase; in the case of mortars exposed to a temperature of 250 °C, a lower correlation coefficient value was obtained (~0.51), which confirms the influence of temperature on the linearity of the relationship between these two variables. The values obtained for UPV value of expanded clay mortar are high for their bulk density (marked with a red circle); this should be due to the characteristics of this specific aggregate, which, despite having a reduced density, provides a high compactness and good bond between the aggregate and the matrix [67].

The Young's modulus and the bulk density can be related by a power law, as illustrated in Figure 9. Correlation coefficients between 0.86 and 0.92 were obtained for the different exposure temperatures, suggesting a high correlation between the two properties even after exposure to elevated temperatures; the more compact mortars (i.e., having a higher density) tend to be more rigid (less deformable) and vice versa.

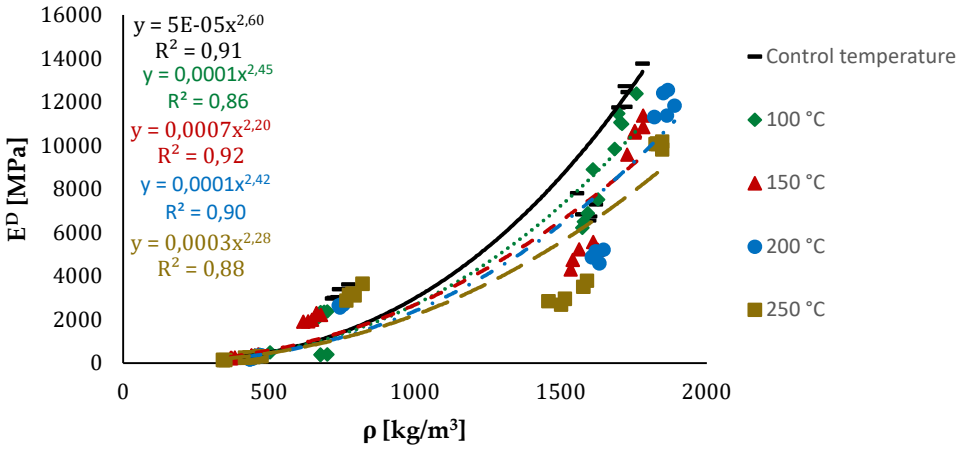

Figure 9. Relationship between bulk density and Young's modulus.

The Young's modulus can also be related to the UPV according to a power law, as shown in Figure 10. This figure indicates that for the studied mortars very high correlation coefficients were obtained between the two variables, between 0.92 and 0.98. It can also be concluded that the correlation coefficient between these two properties was insensitive to the exposure to elevated temperatures.

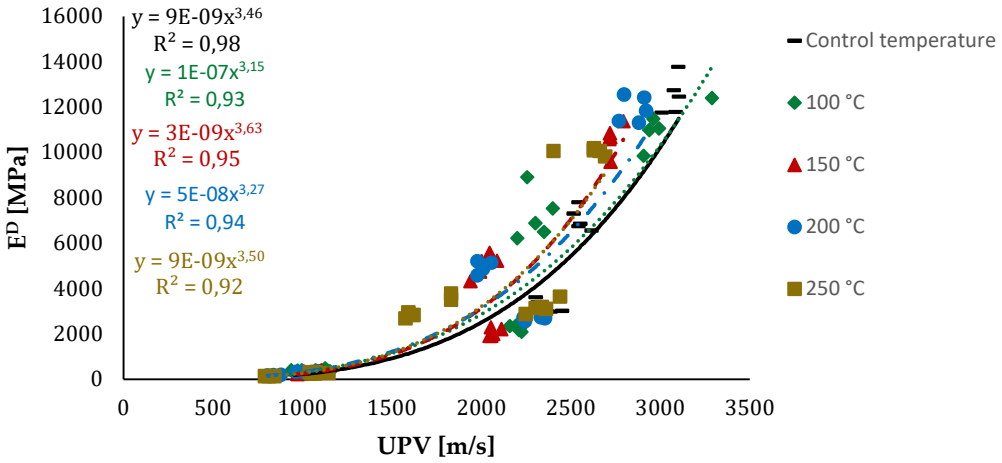

Figure 10. Relationship between ultrasound pulse velocity and Young's modulus.

As shown in Figure 11, there is also a good power correlation between the compressive strength and the bulk density in the hardened state, with correlation coefficients between 0.86 (100 °C) and 0.92 (150 °C). In addition, as shown in Figure 12, there is a very strong power correlation (R^2 ranging from 0.92 and 0.98) between the UPV and compressive strength for the different temperatures. This result is logical and was expected, since compressive strength was indirectly estimated from the Young' modulus, which was also shown to be strongly correlated with UPV.

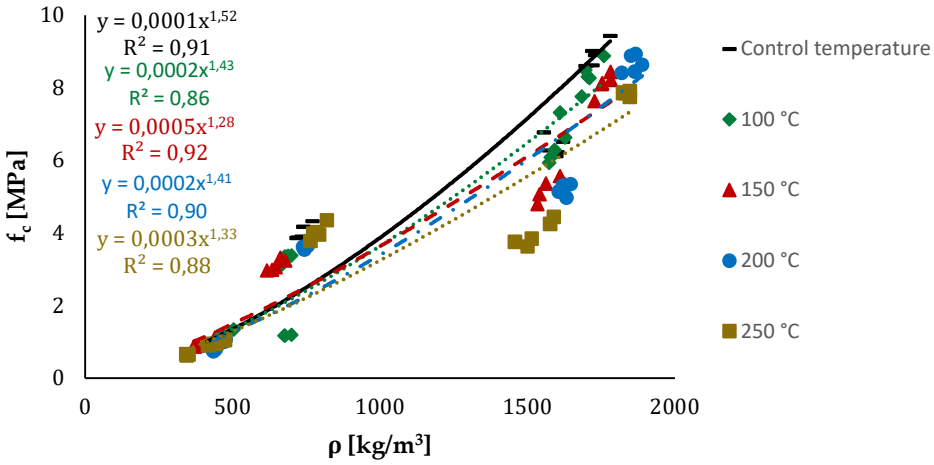

Figure 11. Relationship between bulk density and compressive strength.

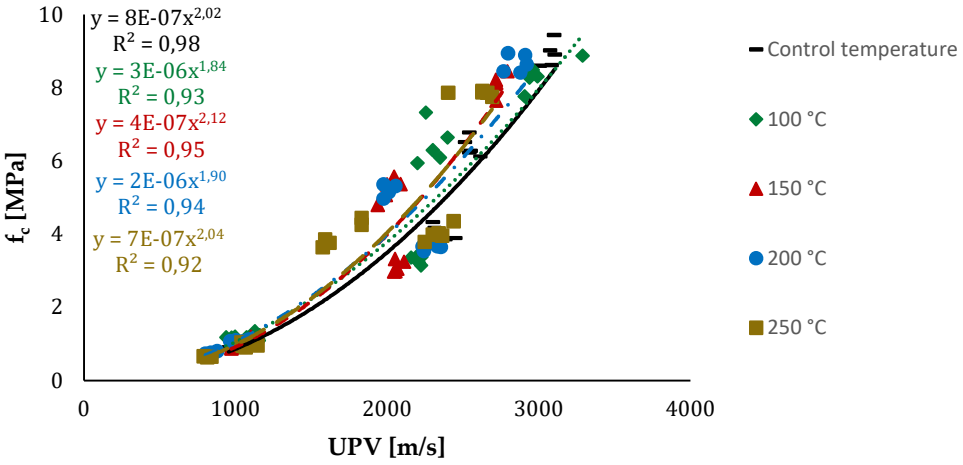

Figure 12. Relationship between ultrasound pulse velocity and compressive strength.

Figure 13 shows a power correlation between the bulk density and the thermal conductivity; the correlation coefficient is higher than 0.97. The lightweight mortars present the lowest density, as well as the lowest thermal conductivity coefficients. However, for a high variation in bulk density of lightweight mortars (350 to 790 kg/m^3) a small variation of thermal conductivity was registered (0.06 to 0.202 W/(m.K)); this shows the difficulty to decrease the thermal conductivity of mortars to reach the performance of thermal insulating materials, which should present thermal conductivity below 0.07 W/(m.K) [68].

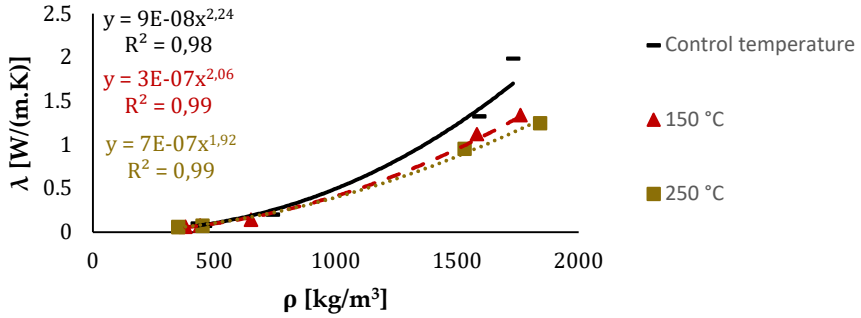

Figure 13. Relationship between bulk density and thermal conductivity coefficient.

Regarding the relation between the mortars' thermal conductivity and UPV (Figure 14), an acceptable correlation was also found, with a correlation coefficient higher than 0.72.

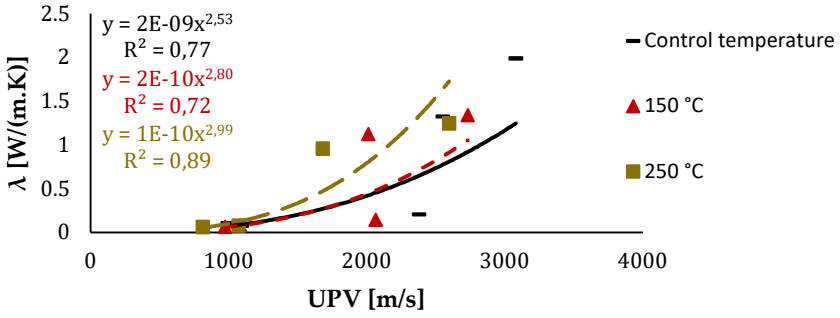

Figure 14. Relationship between ultrasound pulse velocity and thermal conductivity coefficient.

A linear correlation is observed between the thermal conductivity and the Young's modulus (Figure 15), with correlation coefficients of 0.95, 0.86 and 0.81 for the control temperature, 150 °C and 250 °C, respectively. Figure 16 shows the influence of temperature on the relationship between the thermal conductivity and compressive strength. In this case, the values of the linear correlation coefficient vary between 0.89 and 0.91.

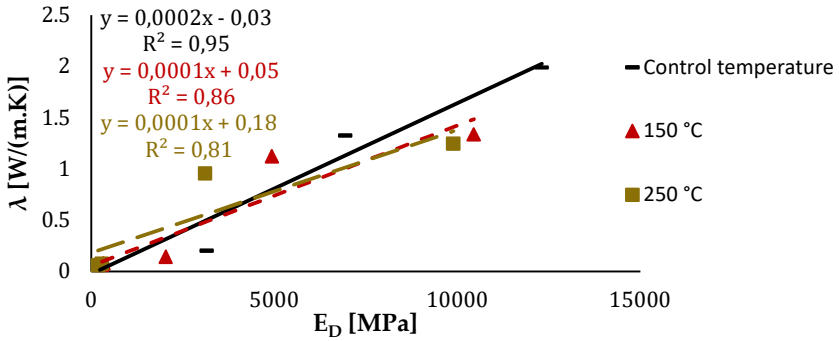

Figure 15. Relationship between Young's modulus and thermal conductivity.

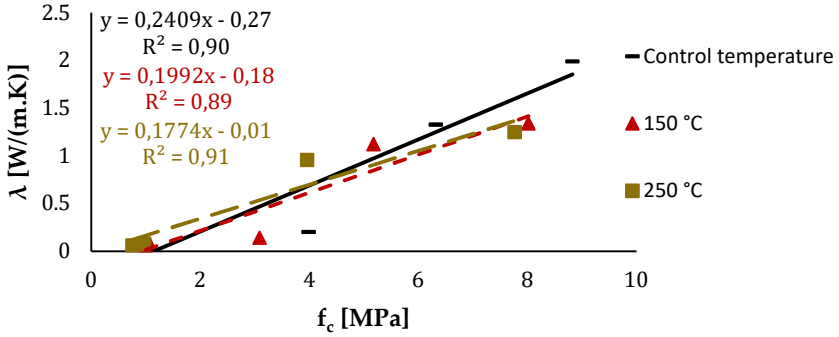

Figure 16. Relationship between compressive strength and thermal conductivity.

The results presented above show that in general there is a good correlation between the thermal conductivity and bulk density, UPV, Young's modulus and compressive strength, even after the mortars are exposed to elevated temperatures. Thus, these correlations can be used in the assessment of thermal mortars exposed to elevated temperature. As mentioned, as a general rule, less compact mortars with less deformation capacity are those with lower bulk density, more voids and, consequently, with lower thermal conductivity. The effects of elevated temperature on mortars depend on the constituent materials (aggregates and cement-paste); however, although exposure to elevated temperature may change (moderately) the values of the correlation coefficients, the overall relations between parameters seem to remain.

4. Conclusions

This paper presented an experimental study about the effects of exposure to elevated temperature on the remaining properties of mortars produced with different insulating aggregates. In general, the physical and mechanical behavior of the thermal mortars was influenced by such exposure: the results obtained, together with the properties of the aggregates (reported in the literature), show that the variation of the mechanical behavior of the thermal mortars (increase and decrease of mechanical strength) is mainly due to the effect of temperature on the cement paste. In addition, the changes in aggregate porosity due to temperature exposure may cause changes in the mechanical strength of the mortars, as is the case of expanded clay.

The results obtained also show that the most sensitive mortars to the effect of temperature are the ones with admixtures (C^{AERO} and E^{AD}). Regarding aerogel mortar (C^{AERO}), despite incorporating

an aggregate that resists to high temperatures *per se*, its binder paste, which incorporates admixtures, led to a worse performance after exposure to high temperatures. This behavior is confirmed by the worse performance of the sand mortar with admixtures (E^{AD}), when compared to the reference mortar (D^{ref}) without admixtures. Even so, mortar with aerogel was the one that showed the lowest variation in thermal conductivity with increasing temperature.

The exposure to high temperatures had a reduced influence on the correlations between different physical and mechanical properties of the mortars studied; this shows that in general exposure to elevated temperature affects the properties of the mortars in a similar way.

Overall, the results obtained show that the mortars with thermal insulation properties studied in this paper are suitable for application in exterior and interior wall coverings. Although they tend to maintain their insulating characteristics when exposed to high temperatures, they undergo internal changes that affect their mechanical strength when exposed to temperatures of 100 ºC and above.

In summary, after being exposed to elevated temperatures, the thermal mortars were able to maintain their insulating characteristics, but experienced internal damage and reduction of their mechanical properties. Therefore, in the case of current exposure to elevated temperatures (e.g., in specific industrial applications), it may be necessary to incorporate specific materials (e.g., additions) in these mortars in order to guarantee enhanced resistance to high temperatures.

Author Contributions: M. Cunha Pereira did the experimental program and wrote the first draft of the paper; A. Soares improved the paper, namely the literature review and the discussion of results; I. Flores-Colen supervised the experimental work, reviewed and edited the paper; J.R. Correia supervised the work and reviewed the paper. All authors have read and agreed to the published version of the manuscript.

Funding: This research was funded by FCT grant PTDC/ECM/118262/2010, NANORENDER research project.

Acknowledgments: The authors acknowledge the financial support provided by CERIS research center, FCT (Foundation for Science and Technology) and COMPETE 2020: FCT Project PTDC/ECM/118262/2010, NANORENDER (2012-2015); FCT PhD Grant SFRH/BD/97182/2013; COMPETE 2020 Project ''PEP—Parede Eficiente Plus'' (POCI-01-0247-FEDER-017417). The authors also acknowledge the following manufacturers and companies: Weber, Argex, Corticeira Amorim and SECIL.

Conflicts of Interest: The authors declare no conflicts of interest.

References

1. European Union. *Directive 2002/91/EC of European Parliament and of the Council of 16 December 2002 on the Energy Performance of Buildings*; 4.1.2003, L 1/65-L 1/71; European Union: Brussels, Belgium, 2002.
2. European Union. *Directive 2010/31/EU of European Parliament and of the Council of 19 May 2010 on the Energy Performance of Buildings*; 18.6.2010, L 153/13-L 153/35; European Union: Brussels, Belgium, 2010.
3. REH. *Energy Performance of Residential Buildings Regulation* (*REH*); Decreto-Lei 118/2013 de 20 Agosto, Portaria n 349-B/2013 de 29 Novembro; INCM: Lisboa, Portugal, 2013. (In Portuguese)
4. Grunewald, J.; Will, T. Pilot Study on the Model Project of the Saxon State Ministry of the Interior: Energetic: Energetic Refurbishment of Architectural Monuments; Technische Universität Dresden—Fakultät Architektur, Dresden: Dresden, Germany, 2010; p. 127. (In German).
5. Garrido, R.; Silvestre, J.; Flores-Colen, I. Economic life cycle assessment of thermal renders. In Proceedings of the 3rd European Mortar Summit, Lisbon, Portugal, 21–22 May 2015.
6. Koebel, M.; Rigacci, A.; Achard, P. Aerogel-based thermal superinsulation: An overview. *J. Sol-Gel Sci. Technol.* **2012**, *63*, 315–339.
7. Comité Européen de Normalisation. *Specification for Mortar for Masonry—Part 1: Rendering and Plastering Mortar*; EN 998-1.; Comité Européen de Normalisation: Brussels, Belgium, 2010.
8. Barbero, S.; Dutto, M.; Ferrua, C.; Pereno, A. Analysis on existent thermal insulating plasters towards innovative applications: Evaluation methodology for a real cost-performance comparison. *Energy Build* **2014**, *77*, 40–47.
9. Comité Européen de Normalisation. *Concrete*: *Specification*, *Performance*, *Production and Conformity*; EN 206-1; Comité Européen de Normalisation: Brussles, Belgium, 2000.
10. Comité Européen de Normalisation. *EN 13055-1*, *Lightweight Aggregates. Lightweight Aggregates for Concrete*, *Mortar and Grout*; Comité Européen de Normalisation: Brussels, Belgium, 2002.

11. Nóvoa, P.; Ribeiro, M.; Ferreira, A.; Marques, A. Mechanical characterization of lightweight polymer mortar modified with cork granulates. *Compos. Sci. Technol*. **2004**, *64*, 2197–2205.
12. Soares, A.; Júlio, M.; Flores-Colen, I.; Ilharco, L.; de Brito, J.; Martinho, J. Water-Resistance of mortars with lightweight aggregates. *Key Eng. Mater.* **2015**, *634*, 46–53.
13. Panesar, D.; Shindman, B. The mechanical, transport and thermal properties of mortar and concrete containing waste cork. *Cem. Concr. Compos*. **2012**, *34*, 982–992.
14. Riffat, S.; Qiu, G. A review of state-of-the-art aerogel applications in buildings. *Int. J. Low-Carbon Technol*. **2013**, *8*, 1–6.
15. Brás, A.; Leal, M.; Faria, P. Cement-cork mortars for thermal bridges correction. Comparison with cement-EPS mortars performance. *Constr. Build. Mater*. **2013**, *49*, 315–327.
16. Bartolini, R.; Filippozzi, S.; Princi, E.; Schenone, C.; Vicini, S. Acoustic and mechanical properties of expanded clay granulates consolidated by epoxy resin. *Appl. Clay Sci.* **2010**, *48*, 460–465.
17. Kalhori, E.; Yetilmezsoy, K.; Uygur, N.; Zarrabi, M.; Shmeis, R. Modeling of adsorption of toxic chromium on natural and surface modified lightweight expanded clay aggregate (LECA). *Appl. Surf. Sci.* **2013**, *287*, 428–442.
18. Vašina, M.; Hughes, D.; Horoshenkov, K.L.L., Jr. The acoustical properties of consolidated expanded clay granulates. *Appl. Acoust.* **2006**, *67*, 787–796.
19. Ebert, H.-P. *Thermal Properties of Aerogels*, *Aerogels Handbook*; Springer: London, UK, 2011; pp. 537–564.
20. Hüsing, N.; Schubert, U. Aerogels—Airy Materials: Chemistry, Structure, and Properties. *Angew. Chem. Int. Ed.* **1998**, *37*, 22–45.
21. Ilharco, L.; Fidalgo, A.; Farinha, J.; Martinho, J.G.; Rosa, M. Nanostructured silica/polymer subcritical aerogels. *J. Mater. Chem*. **2007**, *19*, 2195–2198.
22. Kim, S.; Seo, J.; Cha, J.; Kim, S. Chemical retreating for gel-typed aerogel and insulation performance of cement containing aerogel. *Constr. Build. Mater.* **2013**, *40*, 501–505.
23. Ibrahim, M.; Wurtz, E.; Biwole, P.H. Hygrothermal performance of exterior walls covered with aerogel-based insulating rendering. *Energy Build*. **2014**, *84*, 241–251.
24. Soares, A.; Júlio, M.; Flores-Colen, I.; Ilharco, L.; de Brito, J. EN 998-1 performance requirements for thermal aerogel-based renders. *Constr. Build. Mater.* **2018**, *179*, 453–460.
25. Fu, X.; Chung, D. Effects of silica fume, latex, methylcellulose, and carbon fibres on the thermal conductivity and specific heat of cement paste. *Cem. Concr. Res*. **1997**, *27*, 1799–1804.
26. Patural, L.; Marchal, P.; Govin, A.; Grosseau, P.; Ruot, B.; Devès, O. Cellulose ethers influence on water retention and consistency in cement-based mortars. *Cem. Concr. Res.* **2011**, *41*, 46–55.
27. Cunha, S.; Carneiro, L.; Aguiar, J.; Pacheco-Torgal, F.; Ferreira, V.; Tadeu, A. Behaviour of mortars with the incorporation of phase change materials when exposed to elevated temperatures, In Proceedings of the 1st Luso-Brazilian Congress of Sustainable Building Materials, Braga, Portugal, 5–7 March 2014; pp. 71–83. (In Portuguese)
28. Panias, D.; Balomenos, E.; Sakkas, K. The fire resistance of alkali-activated cement-based concrete binders, Handbook of Alkali-Activated Cements. *Mortars Concr.* **2015**, 423–461, doi:10.1533/9781782422884.3.423.
29. Lorenzoni, R.; Paciornik, S.; Silva, F. Characterization by microcomputed tomography of class G oil well cement paste exposed to elevated temperatures. *J. Petrol. Sci. Eng.* **2019**, *175*, 896–904.
30. Handoo, S.K.; Agarwal, S.; Agarwal, S.K. Physicochemical, mineralogical, and morphological characteristics of concrete exposed to elevated temperatures. *Cem. Concr. Res.* **2000**, *32*, 1009–1018.
31. Cüllfik, M.; Özturan, T. Effect of elevated temperatures on the residual mechanical properties of high-performance mortar. *Cem. Concr. Res.* **2002**, *32*, 809–816.
32. Lion, M.; Skoczylas, F.; Lafhaj, Z.; Sersar, M. Experimental study on a mortar. Temperature effects on porosity and permeability. Residual properties or direct measurements under temperature. *Cem. Concr. Res.* **2005**, *35*, 1937–1942.
33. Ameri, F.; Shoaei, P.; Zareei, S.A.; Behforouz, B. Geopolymers vs. alkali-activated materials (AAMs): A comparative study on durability, microstructure, and resistance to elevated temperatures of lightweight mortars. *Constr. Build. Mater.* **2019**, *222*, 49–63.
34. Guelmine, L.; Hadjab, H.; Benazzouk, A. Effect of elevated temperatures on physical and mechanical properties of recycled rubber mortar. *Constr. Build. Mater*. **2016**, *126*, 77–85.
35. Correia, J.R.; Marques, A.M.; Pereira, C.M.C.; de Brito, J. Fire reaction properties of concrete made with recycle rubber aggregate. *Fire Mater.* **2012**, *36*, 139–152.

36. Comité Européen de Normalisation. *EN 1015-2*, *Methods of Test for Mortar for Masonry—Part 2: Bulk Sampling of Mortars and Preparation of Test Mortars*; Comité Européen de Normalisation: Brussels, Belgium, 1998.
37. Comité Européen de Normalisation. *EN 1015-3*, *Methods of Test for Mortar for Masonry—Part 3: Determination of Consistence of Fresh Mortar* (*by Flow Table*); Comité Européen de Normalisation: Brussels, Belgium, 1999.
38. Gomes, R.; Veiga, M.R.; de Brito, J. The Influence of Execution Procedures in Common Renders. In Proceedings of the 1st National Congress of Building Mortars, APFAC, Lisbon, Portugal, 24–25 November 2005. (In Portuguese)
39. Comité Européen de Normalisation. *EN 1015-11*, *Methods of Test for Mortar for Masonry—Part 11: Determination of Flexural and Compressive Strength of Hardened Mortar*; Comité Européen de Normalisation: Brussels, Belgium, 1999.
40. American Society for Testing Materials. *ASTM 1876-01*, *Standard Test Method for Dynamic Young's Modulus*, *Shear Modulus*, *and Poisson's Ratio by Impulse Excitation of Vibration*; American Society for Testing Materials: Philadelphia, PA, USA, 2009.
41. Silva, A.; Soares, A.; Flores-Colen, I.; de Brito, J. Mechanical characterization of lightweight mortars on small-scale samples. *J. Test. Eval*. **2016**, *44*, 402–413.
42. Silva, A.; Soares, A.; Flores-Colen, I.; de Brito, J. Evaluation of mechanical properties of coating mortars through Young's modulus. Testing on small specimens. In Proceedings of the 5th Conference on Building Pathology and Rehabilitation (PATORREB 2015), Porto, Portugal, 26-28 March 2015. (In Portuguese)
43. Comité Européen de Normalisation. *EN 1015-10*, *Methods of Test for Mortar for Masonry—Part 10: Determination of Dry Bulk Density of Hardened Mortar*; Comité Européen de Normalisation: Brussels, Belgium, 1999.
44. Comité Européen de Normalisation. *EN 12504-4*, *Testing Concrete—Part 4: Determination of Ultrasonic Pulse Velocity*; Comité Européen de Normalisation: Brussels, Belgium, 2004.
45. American Society for Testing Materials. *ASTM D5930-09*, *Thermal Conductivity of Plastics by Means of a Transient Line-Source Technique*; American Society for Testing Materials: Philadelphia, PA, USA, 2009.
46. ISOMET. *Thermal Properties Analyzer. User's Guide*; ISOMET 2114, Version 120712, Applied Precision; ISOMET: Manassas, VA, USA, 2011.
47. Diederichs, U.; Jumppanen, U.-M.; Penttala, V. *Behaviour of High Strength Concrete at High Temperatures*; Report 92; Helsinki University of Technology, Department of Structural Engineering: Espoo, Finland, 1989; Volume 76.
48. Hager, I. Behaviour of cement concrete at high temperature. *Bull. Pol. Acad. Sci. Technol. Sci.* **2013**, *61*, 10.
49. Naus, D. The effect of elevated temperatures on concrete materials and structures—A literature review. *Oak Ridge Natl. Lab.* **2006**, *41*, 184.
50. Chandra, S.; Berntsson, L. *Lightweight Aggregate Concrete*; Noyes Publications/William Andrew Publishing: Norwich, NY, USA, 2002; p. 368.
51. Tantawy, M. Effect of high temperatures on the microstructure of cement paste. *J. Mater. Sci. Chem. Eng.* **2017**, *5*, 33–45.
52. Tufail, M.; Shahzada, K.; Gencturk, B.; Wei, J. Effect of elevated temperature on mechanical properties of limestone, quartzite and granite concrete. *Int. J. Concr. Struct. Mater.* **2017**, *11*, 17–28.
53. Cruz, C.; Gillen, M. Thermal expansion of Portland cement paste, mortar and concrete at high temperatures. *Fire Mater.* **1980**, *4*, 66–70.
54. Deschner, F.; Lothenbach, B.; Winnefeld, F.; Neubauer, J. Effect of temperature on the hydration of Portland cement blended with siliceous fly ash. *Cem. Concr. Res.* **2013**, *52*, 169–181.
55. Fortes, M.A.; Rosa, M.E.; Pereira, H. *The Cork*; IST Press: Lisbon, Portugal, 2004. (In Portuguese)
56. Phan, L. *Fire Performance of High-Strength Concrete: A Report of the State-of-the-Art*; NISTIR 5934; United states department of Commerce Technology Administration, National Institute of Standards and Technology: Gaithersburg, MD, USA, 1996, p. 105.
57. Krishna, D.A.; Priyadarsini, R.; Narayanan, S. Effect of elevated temperatures on the mechanical properties of concrete. In Proceedings of the 2nd International Conference on Structural Integrity and Exhibition Procedia Structural Integrity, Madeira, Portugal, 2–5 September 2019; pp. 384–394.
58. Morsy, M.; Rashad, A.; Shebl, S. Effect of elevated temperature on compressive strength of blended cement mortar. *Build. Res. J.* **2008**, *56*, 173–185.
59. Yusuf, S.; Shafigh, P.; Ibrahim, Z.; Hashim, H.; Panjehpour, M. Crossover effect in cement-based materials: A review. *Appl. Sci.* **2019**, *9*, 2776.

60. Mydin, M.; Wang, Y. Mechanical properties of foamed concrete exposed to high temperatures. *Constr. Build. Mater.* **2012**, *26*, 638–654.
61. CEB; FIP. *Lightweight Aggregate Concrete—CEB/FIP Manual of Design and Technology, Comité Euro-International du Béton, Fédération Internationale de la Précontrainte*; The Construction Press Ltd.: Belfast, UK, 1977.
62. Gross, J.; Fricke, J. Thermal expansion of carbon and silica aerogels above room temperature. *J. Non-Cryst. Solids* **1995**, *186*, 301–308.
63. Gil, L.C. *Materials for Construction and Civil Engineering*; Springer International Publishing: Heidelberg, Germany, 2015; Volume 13, pp. 585–627.
64. Pereira, H. *Cork: Biology, Production and Uses*; Elsevier: Amsterdam, The Netherlands, 2007; p. 160.
65. Magalhães, A.C.; Costa, D.; Veiga, M.R. Anomaly diagnosis of wallcovering with in-situ testing techniques. Evaluation of mechanical strength, In Proceedings of the 3th Meeting on Building Conservation and Rehabilitation (ENCORE), Laboratório Nacional de Engenharia Civil (LNEC), Lisbon, Portugal, 26-30 May 2003; pp. 419–427. (In Portuguese)
66. Raheem, S.; Saheb, M.; Alshreefi, R.; Moula, H.; Maula, B.; Mikhael, Q. Predicting the mechanical features of cement mortar using destructive and non-destructive tests. In Proceedings of the 2nd International Conference on Sustainable Engineering Techniques ICSET, Baghdad, 6-7 March 2019.
67. Lo, T.; Cui, H. Effect of porous lightweight aggregate on strength of concrete. *Mater. Lett.* **2004**, *58*, 916–919.
68. Germany Institute for Standardization. *DIN 4108-2, Thermal Protection and Energy Economy in Buildings—Part 2: Minimum Requirements for Thermal Insulation*; Germany Institute for Standardization: Berlin, Germany, 2003.